THE JOURNAL OF IMMUNOLOGY

Molecular Determinants of Agonist and Antagonist Signaling through the IL-36 Receptor

Sebastian Günther and Eric J. Sundberg

J Immunol 2014; 193:921-930; Prepublished online 16 June 2014;
doi: 10.4049/jimmunol.1400538
http://www.jimmunol.org/content/193/2/921

The Journal of Immunology is published twice each month by
The American Association of Immunologists, Inc.,
9650 Rockville Pike, Bethesda, MD 20814-3994.

Print ISSN: 0022-1767 Online ISSN: 1550-6606.

Molecular Determinants of Agonist and Antagonist Signaling through the IL-36 Receptor

Sebastian Günther* and Eric J. Sundberg*,†,‡

The IL-1 family consists of 11 cytokines that control a complex network of proinflammatory signals critical for regulating immune responses to infections. They also play a central role in numerous chronic inflammatory disorders. Accordingly, inhibiting the activities of these cytokines is an important therapeutic strategy for treating autoimmune diseases and lymphomas. Agonist cytokines in the IL-1 family activate signaling by binding their cognate receptor and then recruiting a receptor accessory protein. Conversely, antagonist cytokines bind their cognate receptor but prohibit recruitment of receptor accessory protein, which precludes functional signaling complexes. The IL-36 subfamily of cytokines is the most diverse, including three agonists and at least one antagonist, and is the least well-characterized group within this family. Signaling through the IL-36 receptor directly stimulates dendritic cells and primes naive CD4 T cells for Th1 responses. Appropriately balanced IL-36 signaling is a critical determinant of skin and lung health. IL-36 signaling has been presumed to function analogously to IL-1 signaling. In this study, we have defined molecular determinants of agonist and antagonist signaling through the IL-36 receptor. We present the crystal structure of IL-36γ, which, to our knowledge, is the first reported structure of an IL-36 agonist. Using this structure as a guide, we designed a comprehensive series of IL-36 agonist/antagonist chimeric proteins for which we measured binding to the IL-36 receptor/IL-1 receptor accessory protein complex and functional activation and inhibition of signaling. Our data reveal how the fine specificity of IL-36 signaling is distinct from that of IL-1. ***The Journal of Immunology*****, 2014, 193: 921–930.**

Almost 30 years ago, the cloning of IL-1α (1) and IL-1β (2) enabled the thorough analysis of their biological functions. Since then, it has been shown that the dysregulation of IL-1 cytokine activities causes a variety of inflammatory disorders (e.g., familial Mediterranean fever, gout, type 2 diabetes), and IL-1 cytokines and receptors have been targeted for numerous indications (3).

Based on sequence and structural similarity, the family of IL-1 cytokines has expanded over time and now consists of eleven cytokines that can be grouped according to their primary receptor (4). IL-1R binds to two activating cytokines, IL-1α and IL-1β, and one inhibitory cytokine, IL-1R antagonist (IL-1Ra). ST2 is the receptor for IL-33, an agonist cytokine, but has no known antagonist. IL-18R binds the agonist IL-18 and the antagonist IL-37. IL-36R (formerly IL-1Rrp2) is the most promiscuous primary receptor with three agonists, IL-36α, IL-36β, and IL-36γ, and one antagonist, IL-36R antagonist (IL-36Ra). Moreover, IL-38 has recently also been described to act as an antagonist for IL-36R in an *Aspergillus* infection model (5).

After binding to their cognate primary receptors, all agonistic ILs recruit the IL-1R accessory protein (IL-1RAcP), except for IL-18, which uniquely recruits the IL-18R accessory protein. Cytokine-mediated dimerization of the primary receptor with the accessory protein drives productive signaling through engagement of cytoplasmic Toll/IL-1 receptor domains from each of these membrane-spanning proteins, ultimately leading to NF-κB or MAPK activation (6). Antagonist cytokines are thought to inhibit signaling by binding to their cognate receptor and preventing the recruitment of the relevant accessory protein.

The IL-36 cytokines are the least well-characterized within the IL-1 family of cytokines, as only recently it has been possible to define the biological functions of these cytokines. For other members of this family it had previously been shown that they act not only on innate immune cells but also stimulate the adaptive immune system. For example, IL-1β increases the lineage commitment of Th17 cells, whereas IL-18 is connected with Th1 cell development and IL-33 with Th2 cell development (7). After the discovery that the IL-36 cytokines require a precisely processed N terminus for high-affinity binding to their cognate receptor IL-36R (8), it was shown that they can directly stimulate bone marrow–derived (9) and monocyte-derived dendritic cells (10). Additionally, naive CD4 T cells express IL-36R and become primed for Th1 responses (11).

A consistent theme in IL-1 family cytokine signaling is the balance between agonism and antagonism that leads to appropriate control of innate immunity and inflammation. Many chronic inflammatory conditions result from an imbalance in activating versus inhibitory signals but can, in some cases, be treated by restoring molecular brakes to signaling in the form of agonist-neutralizing molecules (e.g., Abs or decoy receptors) or engineered antagonists (3, 12). Appropriately balanced signaling through IL-36R is a critical determinant of skin and lung health, as epithelial cells secrete IL-36 cytokines. Overexpression of IL-36α in a mouse model exhibited a similarity to human psoriasis, and deletion of IL-36Ra increased the severity of this phenotype (13).

*Institute of Human Virology, University of Maryland School of Medicine, Baltimore, MD 21201; †Department of Medicine, University of Maryland School of Medicine, Baltimore, MD 21201; and ‡Department of Microbiology and Immunology, University of Maryland School of Medicine, Baltimore, MD 21201

Received for publication February 26, 2014. Accepted for publication May 8, 2014.

This work was supported by American Asthma Foundation Award 13-0066. Use of the Advanced Photon Source is supported by U.S. Department of Energy (Office of Science, Office of Basic Energy Sciences) Contract DE-AC02-06CH11357.

Address correspondence and reprint requests to Dr. Eric J. Sundberg, University of Maryland School of Medicine, 725 West Lombard Street, Baltimore, MD 21201. E-mail address: esundberg@ihv.umaryland.edu

The online version of this article contains supplemental material.

Abbreviations used in this article: IL-1Ra, IL-1R antagonist; IL-36Ra, IL-36R antagonist; IL-1RAcP, IL-1R accessory protein; PDB, Brookhaven Protein Data Bank; SPR, surface plasmon resonance; TEV, tobacco etch virus.

www.jimmunol.org/cgi/doi/10.4049/jimmunol.1400538

The absolute dependence of psoriasis on IL-36 signaling was later observed in an IL-36R knockout mouse (14). In humans, overexpression of all three agonists has been detected in psoriatic skin lesions (13, 15, 16). Moreover, mutations in the antagonist IL-36Ra have been shown to be responsible for general pustular psoriasis, a life-threatening form of the disease (17, 18). In addition to its involvement in psoriasis, IL-36α has also been shown to cause lung inflammation in mice (19).

How IL-36Ra antagonizes IL-36R activation has been deduced to date primarily by analogy to the well-characterized inhibition and activation of IL-1R signaling by IL-1Ra and IL-1β, respectively. The crystal structures of the ternary complexes of IL-1β in complex with either IL-1RI/IL-1RAcP (20) or IL-1RII/IL-1RAcP (21) revealed a largely identical architecture of the ternary complexes, where binding of IL-1RAcP is achieved using a combined surface of IL-1R and IL-1β. Whereas contacts between IL-1RAcP and the two receptors, IL-1RI and IL-1RII, are largely variable, the interactions between the accessory protein and IL-1β are virtually identical in both complexes. Most contacts between IL-1RAcP and IL-1β are made through residues in the loops connecting β strands 4 and 5 (β4/5) and β11/12, and to a lesser extent to residues on β9. Not surprisingly, the largest structural differences between the agonist IL-1β and the antagonist IL-1Ra are located in these loops (21), providing a structural basis for how IL-1Ra prevents IL-1RAcP from binding. Because the cytokines of the IL-36 family also must recruit IL-1RAcP into a cytokine/receptor/accessory protein ternary complex for functional signaling (22), it has been speculated that the modes of activating and inhibitory signaling through IL-36R are similar to those observed for IL-1 agonist and antagonist cytokines (8, 15).

To gain a better understanding of the underlying molecular basis for IL-36 cytokine signaling through IL-36R, we determined the x-ray crystal structure of human IL-36γ, which, to our knowledge, is the first structure of an agonist cytokine belonging to the IL-36 subfamily. This structure, in combination with the previously solved structure of murine IL-36Ra (23), guided our design of a comprehensive series of IL-36γ/IL-36Ra (both human) chimeric mutants with which we have defined, using both biophysical and functional assays, the fine specificity of agonist and antagonist signaling through the IL-36 receptor.

Materials and Methods

Construct generation

All ILs were cloned into a pET30 expression vector (EMD Millipore) containing an N-terminal hexahistidine tag followed by a tobacco etch virus (TEV) protease recognition site. After protease treatment, the final proteins included residues 18–162 of human IL-36γ (UniProt Q9NZH8) and 2–155 of human IL-36Ra (UniProt Q9UBH0; containing a Val to Ser mutation at position 2 for efficient protease cleavage by TEV) corresponding to the previously described highly active processed forms (8). Loop swaps were introduced by PCR using overlapping oligonucleotides containing the new sequences flanked by sequences of the target site for integration, following a FastCloning PCR procedure (24). Site-directed mutations were introduced following the QuikChange mutagenesis method (Agilent Technologies). Sequences of all proteins used in this study are found in Supplemental Fig. 1.

Expression and purification of ILs

All ILs were expressed in *Escherichia coli* BL21(DE3)pLysS cells induced at an OD_{600} of ~0.6 with 0.1 mM isopropyl β-D-thiogalactoside overnight at 18°C. After sonication, proteins were purified by Ni^{2+}-NTA chromatography. The hexahistidine tag was removed by digestion with 6×His-TEV, both of which were removed by a second Ni^{2+}-NTA chromatography step. Finally, the proteins were purified by gel filtration on a Superdex 200 column either in 10 mM MES (pH 6.5) and 50 mM NaCl for crystallography or in 10 mM HEPES (pH 7.4), 150 mM NaCl, and 2 mM DTT for binding and functional assays.

Expression and purification of IL-36R/IL-1RAcP heterodimers

Human IL-36R and IL-1RAcP were expressed and purified as described (8). Briefly, IL-36R (residues 1–335, UniProt Q9HB29) and IL-1RAcP (residues 1–367, UniProt Q9NPH3) were each cloned as fusion proteins with a C-terminal human IgG1 Fc domain and 6×His tag into pFastBac1 (Life Technologies) and subsequently transfected into Sf9 cells for baculovirus propagation. For protein expression, Sf21 cells growing in Sf-900 serum-free medium supplemented with 2% FBS were simultaneously infected with viruses for IL-36R-Fc and IL-1RAcP–Fc. After 84 h the supernatant was passed over a Sepharose column with immobilized IL-36α (UniProt Q9UHA7; residues 6–158, with a Lys to Ser mutation at position 2). Bound receptor was eluted with 0.1 M glycine (pH 3.0), and collected fractions were immediately neutralized with 1 M Tris (pH 8.0) prior to dialysis against PBS (pH 7.4). When cells were individually infected with baculoviruses for either IL-36R–Fc or IL-1RAcP–Fc alone, yielding homodimeric receptors, no protein bound to the immobilized IL-36α. Only supernatant from doubly infected cells yielded a fraction of heterodimeric IL-36R/IL-1RAcP–Fc receptor pairs capable of binding to the immobilized IL-36α.

Binding analysis

Kinetic parameters and affinities of protein–protein interactions were measured by surface plasmon resonance (SPR) analysis using a Biacore T100 biosensor (GE Healthcare). One thousand response units of protein A from *Staphylococcus aureus* (Sigma-Aldrich) were immobilized on all channels of a CM5 sensor chip. Approximately 200 response units of heterodimeric IL-36R–Fc/IL-1RAcP–Fc was captured on flow cell 2, whereas the first flow cell was used as reference. Binding experiments were carried out in 10 mM HEPES (pH 7.4), 150 mM NaCl, 0.05% (v/v) Tween 20, and 2 mM DTT at 25°C as single cycle kinetic analysis using five concentrations of a 4-fold titration series.

Functional analysis

HEK293T cells were cultured in serum-free FreeStyle F17 medium, supplemented with GlutaMAX and gentamicin (Life Technologies). Cells were transfected with full-length human IL-36R cloned into pcDNA4/TO (Life Technologies) using FugeneHD (Promega). The human IL-8 promoter was used as a reporter gene (8) and cloned into the NanoLuc luciferase reporter vector pNL2.2 (Promega). Both plasmids were transfected at a ratio of 10:1 (reporter/IL-36R). IL-1RAcP is endogenously expressed by HEK293T cells (25). Eighteen hours after transfection, cells were harvested and seeded into a 96-well plate for exposure to ILs. For activation assays, cells were incubated with titrated concentrations of ILs for 5 h prior to cell lysis and measurement of luciferase activity using a Veritas luminescence reader (Promega). Data were normalized to the average activation of wild-type IL-36γ measured at 100 and 1000 nM in each experiment. For inhibition assays, the cells were pretreated for 15 min with antagonist prior to activation by 2 nM IL-36γ. Five hours later, cells were lysed and luciferase activity was measured. Data were normalized to the activity measured in the absence of antagonist. Nonstimulated cells were used for background subtraction. All results shown are the means of duplicates ± SD of representative experiments that were conducted at least three times.

Crystallization and structure determination

IL-36γ was buffer-exchanged into 20 mM MES (pH 6.5) and 150 mM NaCl, concentrated to 10 mg/ml, and crystallized by hanging drop vapor diffusion against 30% (w/v) PEG 5000 MME and 0.1 M sodium acetate (pH 4.5). Crystals were cryo-cooled in mother liquor supplemented with 20% (v/v) ethylene glycol. Data were collected at beam line 12-2 of the Stanford Synchrotron Radiation Lightsource. IL-36Ra(β11/12) was buffer-exchanged into 10 mM HEPES (pH 7.4), 150 mM NaCl, and 2 mM DTT and crystallized by sitting drop vapor diffusion against 1.2 M NaH_2PO_4, 0.6 M K_2HPO_4, 0.1 M CAPS (pH 10.5), and 0.2 M $LiSO_4$. The crystal form was improved by microseeding. Crystals were cryo-cooled in mother liquor supplemented with 20% (v/v) glycerol, and data were collected at beam line 23ID-B of GM/CA at the Advanced Photon Source, Argonne National Laboratory. IL-36Ra(β4/5|β11/12) and IL-36Ra(β4/5|β11/12)$^{R103A/M105A}$ were also buffer-exchanged into 10 mM HEPES (pH 7.4), 150 mM NaCl, and 2 mM DTT concentrated to 10 mg/ml and crystallized by sitting drop vapor diffusion against 25% (w/v) PEG 5000 MME, 0.1 M sodium acetate (pH 5.3) and 30% (w/v) PEG 5000 MME, 0.1 M sodium acetate (pH 5.3), respectively. Crystals were cryo-cooled in mother liquor supplemented with 20% (v/v) glycerol, and data were collected at beam line 11-1 of the Stanford Synchrotron Radiation Lightsource. All data sets were processed using the XDS package (26) and AIMLESS (27). Initial phases were obtained by molecular replacement using the program PHASER (28) using the model of murine IL-36Ra (Brookhaven Protein Data

Bank [PDB] code 1MD6) as a search model. The final models were built using iterative rounds of refinement with the PHENIX program package (29) interspersed with manual model building in COOT (30). The IL-36γ, IL-36Ra(β11/12), IL-36Ra(β4/5|β11/12), and IL-36Ra $(β4/5|β11/12)^{R103A/M105A}$ structures were deposited in the PDB with IDs 4IZE, 4P0J, 4P0K, and 4P0L, respectively.

Results

Crystal structure of IL-36γ

The x-ray crystal structure of the agonist IL-36γ exhibits the typical β-trefoil fold observed in all other IL-1 family ILs, consisting of 12 β-strands connected by 11 loops (Fig. 1, Supplemental Table I). Superposition with the structure of the murine IL-36 antagonist IL-36Ra (23), which has 90.4% sequence identity to human IL-36Ra, reveals a largely identical structure with an overall root mean square deviation of 1.14 Å. The largest differences are located in the β4/5, β6/7, and β11/12 loops.

Activation and inhibition of the IL-36 signaling cascade are assumed to follow the same principles as for IL-1 (8). The structure of IL-36γ allowed us to build a model of the IL-36R/IL-1RAcP/IL-36γ ternary signaling complex with a homology model of IL-36R and the structure of IL-1RAcP from the previously determined IL-1 signaling complexes using these as a blueprint (Fig. 1A). This model shows that the β4/5 and β11/12 loops are likely to directly interact with IL-1RAcP. These two loops exhibit the largest conformational differences between the IL-36γ and IL-36Ra structures (Fig. 1B). The β6/7 loop is not predicted to be involved in binding to either IL-1RAcP or IL-36R. Compared to IL-36γ, the β11/12 loop in IL-36Ra is four amino acids longer, and superposing IL-36Ra onto the ternary complex of IL-1 leads to significant clashes with IL-1RAcP. In contrast, the β4/5 loop is four amino acids shorter, which likely prevents residues from this loop from engaging IL-1RAcP.

Charge effects on binding to IL-1RAcP and IL-36R signaling

In addition to the importance of the β4/5 and β11/12 loops, it has been reported that a charged residue directly C-terminal of the β11/12 loop has a large influence on the agonist and antagonistic properties of IL-1β relative to IL-1Ra (31). In IL-1β this residue is an aspartate (Asp^{145}) (Fig. 1C, Supplemental Fig. 2A). Changing it to lysine, as found in IL-1Ra (Lys^{145}), drastically reduces the agonistic activity of IL-1β, whereas the reverse mutation renders IL-1Ra partially agonistic (31, 32). In the IL-1R complex structures, IL-1β residue Asp^{145} makes a direct hydrogen bond to Ser^{185} of IL-1RAcP (Supplemental Fig. 2A). All IL-36 cytokines except IL-36γ have residues capable of hydrogen bonding at this position (IL-36Ra and IL-36α, aspartate; IL-36β, asparagine, IL-36γ, alanine). That IL-36Ra has an aspartate at this position implies that it is likely using a different strategy, at the atomic level, to inhibit IL-1RAcP binding than does IL-1Ra. In fact, when the structure of IL-36Ra was initially determined, its receptor had not yet unambiguously been identified, and it was thus assumed that it would act as an agonist based on the similarity of this residue to that of IL-1β (23).

To test the importance of this residue for binding and activity of IL-36 cytokines, we mutated it in both IL-36γ (position 162) and IL-36Ra (position 148). In IL-36γ, introduction of an aspartate at position 162 increased the affinity to the preformed IL-36R/IL-1RAcP heterodimer 3-fold, whereas mutating Ala^{162} to lysine reduced the affinity 100-fold, as measured by SPR (Fig. 2A, 2B, Supplemental Table II). We observed parallel effects when we measured signaling through IL-36R in a cell-based functional assay. IL-$36γ^{A162D}$ activated IL-36R signaling similar to wild-type IL-36γ, whereas IL-$36γ^{A162K}$ had an ~15,000-fold reduced activity (Fig. 2C). To determine whether the reduced activity of the IL-

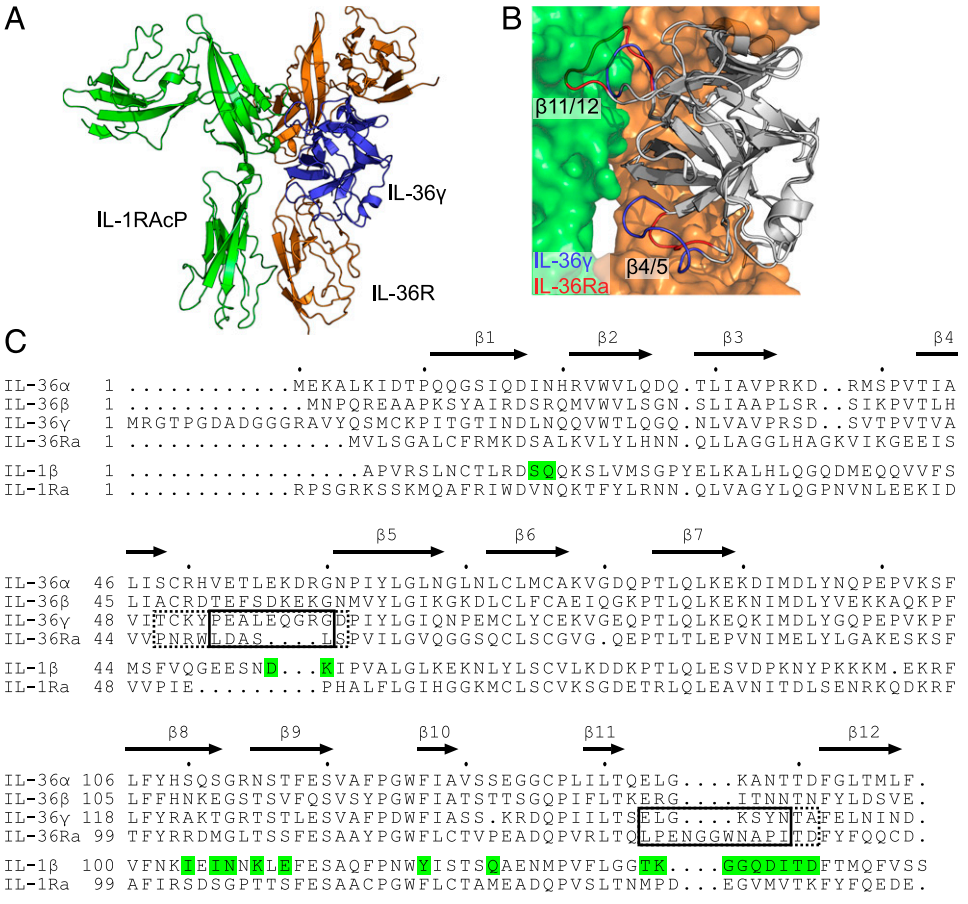

FIGURE 1. Structure of IL-36γ and the IL-36 signaling complex. (**A**) Model of the IL-36 signaling complex containing the crystal structure of IL-36γ. A homology model of IL-36R in complex with the crystal structure of IL-36γ was modeled onto the ternary complex of IL-1RII/IL-1RAcP/IL-1β (PDB 3O4O). (**B**) Comparison of IL-36 agonist and antagonist. The structures of IL-36γ and murine IL-36Ra (PDB 1MD6) were superposed. The surface of IL-36R (orange) and IL-1RAcP (green) based on the model in (A) are depicted and the two loops likely guiding agonism and antagonism are colored in blue (IL-36γ) and red (IL-36Ra). Loop β11/12 of IL-36Ra clashes with IL-1RAcP. (**C**) Structure-guided sequence alignment of IL-36 ILs and IL-1β and IL-1Ra. IL-1β residues interacting with IL-1RAcP based on the available complex structures with IL-1RI/IL-1β (PDB 4DEP) and IL-1RII/IL-1β (PDB 3O4O) are highlighted in green. Loops swapped between IL-36γ and IL-36Ra are indicated (solid line, short loop swaps; dashed line, extended loop swaps).

36γ^{A162K} variant was potentially caused by a gain in antagonist properties, we tested this variant for inhibition of IL-36R signaling (Fig. 2D); however, it did not show any sign of inhibition. In IL-36Ra, changing Asp^{148} to lysine led to no apparent change in IL-36R/IL-1RAcP heterodimer binding affinity (Fig. 2A, 2B, Supplemental Table II) and a similar inhibitory profile to wild-type IL-36Ra (Fig. 2D). At the highest concentration tested in the inhibition assay, we observed a highly reproducible reduction in inhibitory capacity for IL-36Ra^{D148K} relative to wild-type IL-36Ra, likely attributable to cross-reactivity of this mutant with other receptors expressed endogenously by HEK293T cells, as we also observed activation of cells not transfected with IL-36R at high concentrations of IL-36Ra^{D148K}.

In summary, the mutagenesis data for IL-36γ and the conservation of residues putatively functioning as hydrogen bond acceptors in IL-36α (aspartate) and IL-36β (asparagine) suggest a conservation of the three-dimensional orientation of the IL-1RAcP to the IL-36R/IL-36 agonist complex, thus enabling the interaction between Ser^{185} of IL-1RAcP and the IL-36R–bound agonist cytokine. However, it is unclear whether the orientation of the antagonist IL-36Ra in the complex with IL-36R would allow these same interactions, as the potential of aspartate in IL-36Ra to act as a hydrogen bond acceptor may be shielded by the long adjacent β11/12 loop. These data suggest that IL-36Ra is using a different approach than IL-1Ra to inhibit binding of IL-1RAcP.

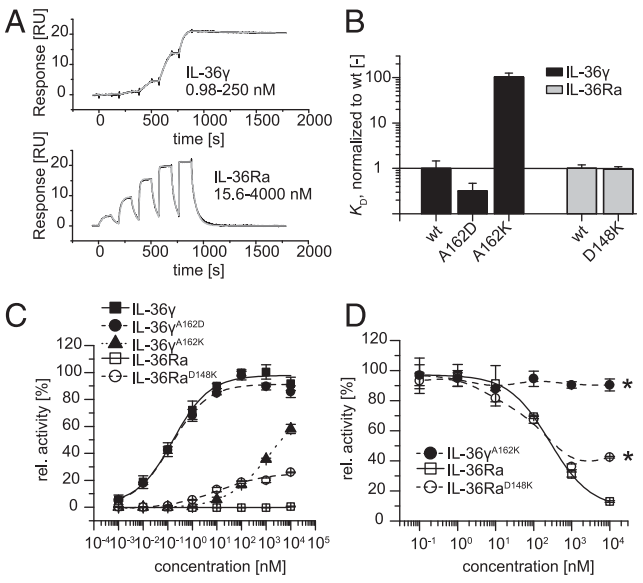

FIGURE 2. Charge effects on binding to IL-1RAcP and IL-36R signaling. (**A**) Representative SPR binding experiments of IL binding to a heterodimeric complex of IL-36R and IL-1RAcP. Black line indicates measured data, gray line fit to a 1:1 binding model. Analyzed concentrations ranges are indicated. (**B**) Comparison of charge-switched mutants. Dissociation constants from SPR binding experiment to IL-36R/IL-1RAcP were normalized to respective wild type proteins (black, IL-36γ, K_D = 0.26 ± 0.12 nM; gray, IL-36Ra, K_D = 67 ± 14 nM). Data are the average of at least five experiments ± SD (exact number of replicates is given in Supplemental Table II). (**C**) Activation of IL-36 signaling by charge-switched mutants. HEK293T cells expressing IL-36R and an IL-8p luciferase reporter gene were stimulated for 5 h with wild-type and mutant IL-36 cytokines prior to measurement of luciferase activity. Maximal stimulation by IL-36γ was set to 100% activity. Data are the means of duplicates ± SD. One representative experiment of three replicates is shown. (**D**) Inhibition of IL-36R signaling by charge-switch mutants. HEK293T reporter cells were treated with titrated amounts of wild-type and mutant IL-36 cytokines. Fifteen minutes after treatment, cells were stimulated for 5 h with 2 nM IL-36γ prior to measurement of luciferase activity. Stimulation in the absence of antagonist was set to 100% activity. Data are the means of duplicates ± SD. One representative experiment of three replicates is shown. All data were fit to a four-parameter function, except those indicated with an asterisk.

β11/12 loop swaps

Next we asked how much the β11/12 loop, directly N-terminal of the aforementioned charged residue, contributes to the activation and/or inhibition of the IL-36R signaling cascade. We swapped the β11/12 loop between IL-36γ and IL-36Ra (Fig. 1C) and assessed their binding to IL-36R/IL-1RAcP heterodimers and abilities to activate and inhibit IL-36R signaling. Two different loop lengths were chosen based on previous results: 1) a shorter version that included only the loop connecting the two β-strands (β11/12), and 2) a longer version that additionally included the residues C-terminal to the loop (β11/12*), including the residues that potentially bind directly to IL-1RAcP as described above. Replacing the β11/12 loop in IL-36γ with that which corresponds to IL-36Ra led to a 14-fold reduction in binding affinity (Fig. 3G, Supplemental Table II) and to a >1000-fold reduced activity (Fig. 3A). The additional inclusion of the Ala^{162}Asp mutation did not increase the affinity as it did in wild-type IL-36γ, but instead reduced it further. This loss in affinity also correlated with a further reduction in agonist activity compared with the shorter β11/12 loop swap (Fig. 3A). In both cases the loss in affinity was mainly caused by an increased dissociation rate (Supplemental Table II). The corresponding changes in IL-36Ra only slightly decreased the affinity for IL-36R/IL-1RAcP (Fig. 3G, Supplemental Table II), which was reflected by marginally reduced antagonism (Fig. 3E).

Taken together, these results imply that the β11/12 loop is much more important for agonist than for antagonist function. When combined with the previous results for the single point mutant IL-36γ^{A162D}, these data indicate that the longer β11/12 loop of IL-36Ra masks the interactions of this residue C-terminal of the loop to the aforementioned helix in IL-1RAcP (Supplemental Fig. 2A).

β4/5 loop swaps

Another region that makes direct contact with IL-1RAcP in the IL-1β ternary complex structures is the β4/5 loop. More specifically, in both cases Asp^{54} of IL-1β, at the tip of its β4/5 loop, forms a hydrogen bond with Arg^{286} of IL-1RAcP (Supplemental Fig. 2B). In IL-36γ, both the length of the loop and its conformation are markedly different (Fig. 1C, Supplemental Fig. 2B, 2C). The two residues closest in space to IL-1β Asp^{54} in IL-36γ are Gly^{70} and Arg^{71}. The arginine makes intramolecular hydrogen bonds with IL-36γ residues Glu^{131} and Asp^{137}, suggesting that it may not be free to engage IL-1RAcP, whereas the glycine is missing a side chain necessary for interaction with IL-1RAcP. Therefore, the mechanism of IL-1RAcP recruitment by the IL-36R/IL-36γ complex must differ from that of the IL-1R/IL-1β complex. At position 70, IL-36α has a glutamate residue and IL-36β an aspartate, such that these IL-36 agonist cytokines could mediate interactions in a ternary complex in a similar fashion as has been observed for IL-1β.

To estimate the general contribution of the IL-36γ β4/5 loop to IL-36R signaling, we conducted the same set of experiments as described above for the β11/12 loop swap mutants. Exchanging the β4/5 loop in IL-36γ reduced its affinity for the preformed IL-36R/IL-1RAcP-Fc complex only slightly (Fig. 3G, Supplemental Table II) and its cell-based activity ~10-fold (Fig. 3C). Compared to the effects of the β11/12 loop, the β4/5 loop makes a relatively small contribution to the interaction with IL-1RAcP. The reverse experiment with IL-36Ra yielded a 2-fold affinity increase (Fig. 3G, Supplemental Table II). This increase in affinity to the IL-36R/IL-1RAcP heterodimer is likely due to increased affinity specifi-

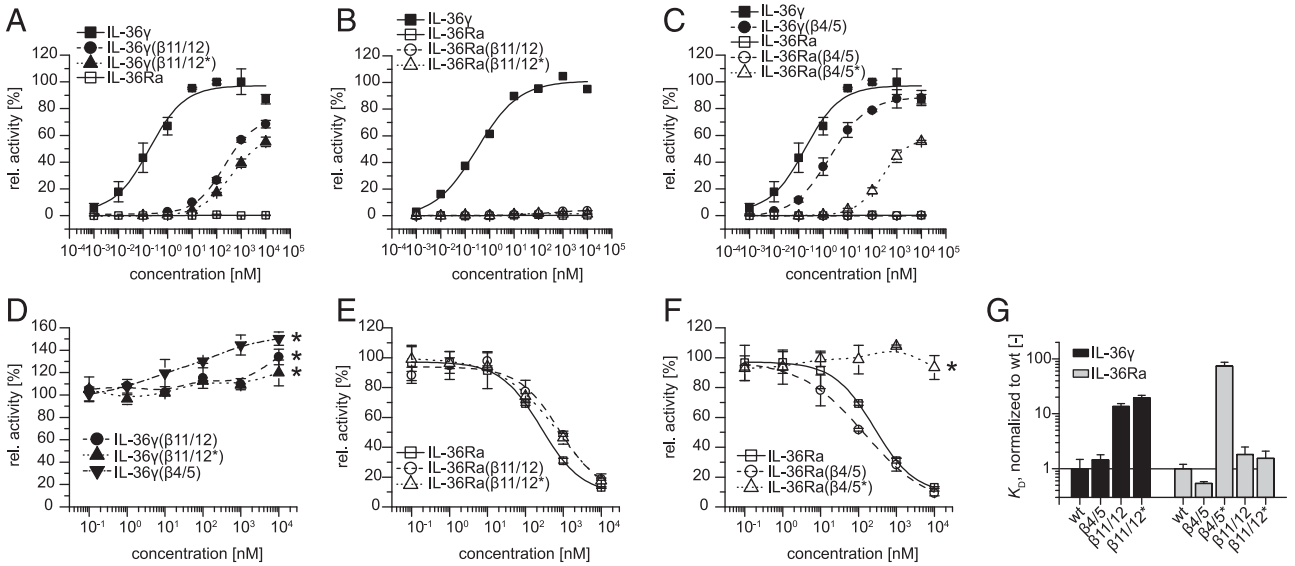

FIGURE 3. Single loop swaps between IL-36γ and IL-36Ra influence binding to and signaling through IL-36R. (**A**–**C**) Activation and (**D**–**F**) inhibition of IL-36 signaling by exchanging loops β11/12 and β4/5 between IL-36γ and IL-36Ra. Impact of exchanging single loops between agonist and antagonist was measured in HEK293T cells expressing IL-36R and an IL-8p luciferase reporter gene as described in Fig. 2. Data are the means of duplicates ± SD. One representative experiment of three replicates is shown. All data were fit to a four-parameter function, except those indicated with an asterisk. (**G**) Comparison of dissociation constants of single loop-swapped variants from SPR binding experiment to IL-36R/IL-1RAcP. Data were normalized to respective wild-type proteins (black, IL-36γ, $K_D = 0.26 \pm 0.12$ nM; gray, IL-36Ra, $K_D = 67 \pm 14$ nM). Data are the averages of at least two experiments ± SD (exact number of replicates is given in Supplemental Table II).

cally to IL-36R, not to IL-1RAcP, as this mutant did not show any agonist properties but, instead, was a better antagonist than wild-type IL-36Ra (Fig. 3F). A possible cause for this observed improved binding is that the introduction of the IL-36γ β4/5 loop alters the electrostatic potential of this region. This, in turn, could influence binding to and, subsequently, mobility of domain 3 (D3) of IL-36R, which is part of the binding interface with IL-1RAcP in the ternary complex structures with IL-1β. Moreover, it has been shown that the linker between D2 and D3 is highly flexible, allowing for numerous positions of D3 relative to D1/D2, which are effectively fixed in position relative to one another (33, 34).

We also designed a second β4/5 loop-swapped IL-36Ra variant (β4/5*) (see Fig. 1C). In this case, the complete loop connecting β strands 4 and 5 was exchanged, resulting in five additional amino acids being exchanged (four on the N-terminal and one on the C-terminal sides). Surprisingly, this loop variant had a >70-fold reduced affinity for the IL-36R/IL-1RAcP complex compared with wild-type IL-36Ra (Fig. 3G, Supplemental Table II), lost all of its antagonist potential, but gained substantial agonist activity (Fig. 3C). In fact, its signaling ability was comparable to the IL-36γ(β11/12) loop-swapped variant, which has the same loops (i.e., β4/5 from IL-36γ and β11/12 from IL-36Ra) (Fig. 3A), although this IL-36Ra variant bound to the IL-36R/IL-1RAcP complex ∼2000-fold weaker. This may be due to the extended loop swap causing more extensive conformational changes in adjacent regions such as the β7/8 loop, which could negatively impact its interaction with IL-36R.

In summary, only five residues around the β4/5 loop appear to be crucial for the antagonistic properties of IL-36Ra, as the shorter loop-swapped version exhibited increased binding and antagonism. Conversely, the extended β4/5 loop-swapped version of IL-36Ra lost this property and became a pure agonist (although with much lower potency than wild-type IL-36γ).

Combining loop swaps increases partial agonist behavior

After assessing the influence of the individual loops, we also characterized variants in which both loops were exchanged. For IL-36γ, exchanging both loops led to a drastic loss in affinity of >30,000-fold (Fig. 4G, Supplemental Table II). This IL-36γ(β4/5|β11/12) variant, however, activated IL-36R signaling as well as did the IL-36γ(β11/12) variant (Fig. 4A). Moreover, this variant exhibited no signs of antagonistic behavior, supporting the likelihood that more sites of interaction between IL-36R–bound IL-36γ and IL-1RAcP exist than just the β4/5 and β11/12 loops. Combining both loop swaps in IL-36Ra resulted in a IL-36R/IL-1RAcP binding affinity equal to the that of wild-type IL-36Ra (Fig. 4G, Supplemental Table II). However, this variant became a partial agonist, stimulating at an activation level of ∼40% of IL-36γ, with nearly no remaining antagonist potential (Fig. 4B, 4E). In contrast, the combination of the β11/12 loop swap with the extended β4/5 loop, which alone led to a 70-fold decrease in affinity for the IL-36R/IL-1RAcP complex, further reduced its affinity to the micromolar range (Fig. 4G, Supplemental Table II). Concomitant with this loss in affinity, the double-swapped IL-36Ra variant exhibited reduced IL-36R–mediated signaling activation and became unable to inhibit signaling by IL-36γ (Fig. 4C, 4F).

Structural integrity of loop-swapped mutants

To ensure the structural integrity of the β4/5 and β11/12 loop-swapped cytokines, we determined the crystal structures of the single loop-swapped IL-36Ra(β11/12) and the double loop-swapped IL-36Ra(β4/5|β11/12). As expected, the structures of the chimeras were almost perfectly superimposable with murine IL-36Ra (23) (root mean square deviation of 1.37 Å for the single and 1.31 Å for the double loop-swapped variants, respectively), except for the loops that had been swapped with the ones from IL-36γ (Supplemental Fig. 2D, Supplemental Table I). The only other loop that adopted a different conformation was loop β7/8. In the murine structure this loop is involved in crystal contacts, whereas in our structures, it is not stabilized by any contacts to neighboring molecules in the crystal. Both exchanged loops adopted a conformation clearly distinct from wild-type IL-36Ra. Comparison with these loops in the IL-36γ structure confirmed that their conformations were maintained in the IL-36Ra chimeras (Supplemental Fig. 2D). In the double loop-swapped structure, notably, IL-36Ra residues N-terminal of the loop also adopted the conformation observed in the wild-type IL-36γ structure (Supplemental Fig. 2C). It is therefore highly

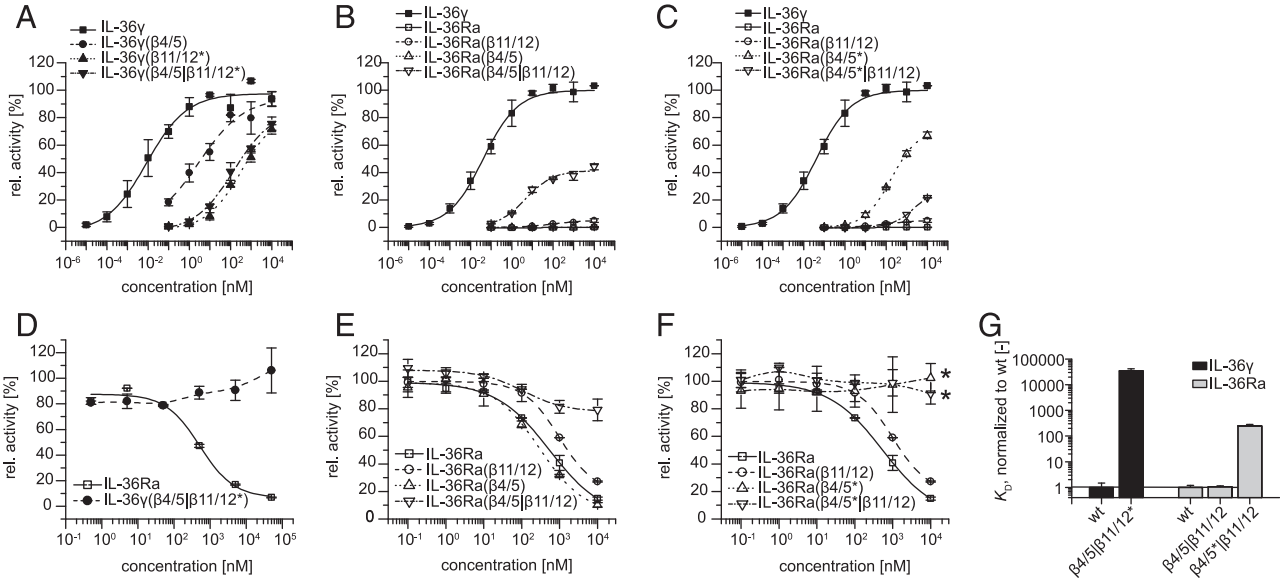

FIGURE 4. Combination of β4/5 and β11/12 loop swaps further modulates activity of IL-36γ and IL-36Ra. (**A**–**C**) Activation and (**D**–**F**) inhibition of IL-36 signaling by simultaneously exchanging loops β11/12 and β4/5 between IL-36γ and IL-36Ra was measured using HEK293T reporter cells as described before in Fig. 2. Data are the means of duplicates ± SD. One representative experiment of three replicates is shown. All data were fit to a four-parameter function, except those indicated with an asterisk. (**G**) Comparison of dissociation constants of double loop-swapped variants from SPR binding experiment to IL-36R/IL-1RAcP. Data were normalized to respective wild-type proteins (black, IL-36γ, $K_D = 0.26 \pm 0.12$ nM; gray, IL-36Ra, $K_D = 67 \pm 14$ nM). Data are the averages of at least three experiments ± SD (exact number of replicates is given in Supplemental Table II).

likely that the extended swap of the β4/5 loop from IL-36γ into IL-36Ra also maintains its original conformation.

These structures enabled us to model the influence of the observed changes on the binding of IL-36Ra to IL-36R. We used the structure of IL-1RI/IL-1β (PDB 4DEP) as a general model for the IL-36R/IL-36 complexes. The homology model of IL-36R was generated using the Web version of Modeler (35). The modeled complex structures of IL-36R with IL-36γ, IL-36Ra(β11/12), and IL-36Ra(β4/5|β11/12) show that the β4/5 loop is proximal to D3 of IL-36R (Supplemental Fig. 2C). Comparison of the loop-swapped IL-36Ra with wild-type IL-36γ and IL-36Ra show that Trp^{49} adopts a different rotamer conformation, which is similar to the rotamer of Tyr^{63} at the corresponding position in wild-type IL-36γ. In the wild-type IL-36Ra β4/5 loop, the amine of the Trp^{49} indole ring forms a hydrogen bond to the main chain of loop β7/8. In its new rotamer position in the IL-36Ra(β4/5|β11/12) chimera, it is rotated away from intramolecular interactions and is, consequently, free to make intermolecular interactions with D3 of IL-36R. This could explain why the chimera IL-36Ra(β4/5) bound better than did wild-type IL-36Ra and was, in fact, a better antagonist.

The fact that the loop swaps of the extended β4/5 loop showed drastically different behavior must be due to the five residues adjacent to this loop that differ between both IL-36Ra variants (see Fig. 1C). Of these five residues, only three residues directly adjacent to the exchanged part form the surface of the IL and have the potential to interact with IL-36R, two of which are on the N-terminal side of the loop and one on the C-terminal side. In IL-36Ra with the extended β4/5 loop swap, Arg^{50} is changed to lysine and Trp^{49} to tyrosine. On the C-terminal side Ser^{55} becomes aspartate. All of these changes could enable new interactions with IL-36R D3, which could influence binding to IL-1RAcP. In the structure of IL-1RI with IL-1Ra, this domain is positioned away from the potential interface with IL-1RAcP when compared with the complex of IL-1RI with IL-1β and the ternary complex of IL-1RII/IL-1β/IL-1RAcP (21, 36, 37). This is likely one cause for the antagonistic properties of IL-1Ra.

Residues on β8 influence IL-1RAcP binding

The fact that exchanging both loops did not turn IL-36Ra into a full agonist, comparable to IL-36γ, indicated that these two loops are not the only sites important for engaging IL-1RAcP. Additional sites that likely contact IL-1RAcP are found on β strands 8 and 9 (Fig. 1A, 1C). The two side chains that would face the predicted IL-1RAcP binding site are Arg^{103} and Met^{105} in IL-36Ra, whereas in IL-36γ these are Ala^{122} and Thr^{124}, two significantly smaller residues. A molecular model of the ternary IL-36 signaling complex indicates that the hydrogen bond between Ser^{185} of IL-1RAcP and the charged residues adjacent to the β11/12 loop of the cytokine could be influenced by residues on β8. That is, Arg^{103} and Met^{105} may sterically hinder the insertion of the IL-1RAcP α helix containing Ser^{185} into a pocket formed by IL-36R/IL-36γ (Supplemental Fig. 2A). Accordingly, mutation of Arg^{103} alone reduced the affinity of the IL-36Ra(β11/12) loop mutant for the IL-36R/IL-1RAcP complex 2-fold (Fig. 5G, Supplemental Table II), the low activation observed for IL-36Ra(β11/12) is further reduced, and no significant change in inhibitory activity was measureable (Fig. 5A, 5D). The double mutant in contrast showed a 2-fold increased affinity, an increase in agonist activity, and at the same time reduced inhibitory activity (Fig. 5A, 5D, Supplemental Table II). This supports the hypothesis that removal of the potential steric clashes caused by these side chains prevents the interaction of Ser^{185} of IL-1RAcP with Asp^{148} of the β11/12 loop-swapped IL-36Ra.

Finally, we included the double mutation Arg^{103}Ala/Met^{105} Ala in the double loop-swapped IL-36Ra variants. Combination of both double loop-swapped IL-36Ra variants (with the shorter and longer β4/5 loop) led to 2- and 6-fold increases in affinity, respectively, for the IL-36R/IL-1RAcP complex (Fig. 5G, Supplemental Table II). For the double-swapped IL-36Ra mutant with the shorter β4/5 loop, this increase in affinity resulted in an increase in antagonistic potential (Fig. 5E), almost reaching the wild-type inhibition level, and simultaneous loss of agonist activity (Fig. 5B). In contrast, the double-swapped variant with the extended β4/5 loop exhibited increased affinity and agonistic

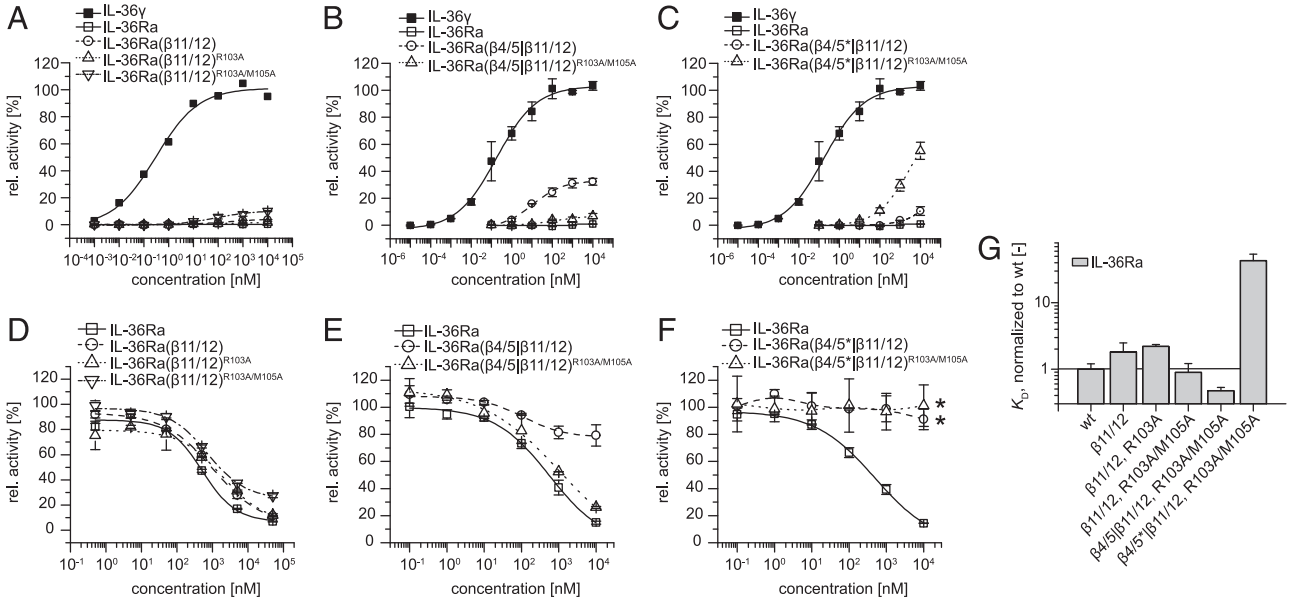

FIGURE 5. Residues on β8 further influence activity of IL-36Ra. (**A**–**C**) Activation and (**D**–**F**) inhibition of IL-36 signaling combining point mutations Arg^{103}Ala and Met^{105}Ala with either single loop-swapped (A and D) or double loop-swapped IL-36Ra (B, C, E, and F) were measured using HEK293T reporter cells as described before in Fig. 2. Data are the means of duplicates ± SD. One representative experiment of three replicates is shown. All data were fit to a four-parameter function, except those indicated with an asterisk. (**G**) Comparison of dissociation constants of IL-36Ra loop-swapped point mutants from SPR binding experiments to IL-36R/IL-1RAcP. Data were normalized to respective wild-type proteins (black, IL-36γ, K_D = 0.26 ± 0.12 nM; gray, IL-36Ra, K_D = 67 ± 14 nM). Data are the averages of at least four experiments ± SD (exact number of replicates is given in Supplemental Table II).

behavior (Fig. 5C, 5G, Supplemental Table II), which is similar to that of the single β4/5* loop-swapped IL-36Ra variant (Fig. 3C). In both β4/5|β11/12 double-swapped chimeras the introduction of the double point mutation led to a molecule whose effect more closely resembled the one from the respective single β4/5 loop-swapped IL-36Ra variants, effectively overriding the combinatorial effect of the β11/12 loop. To better understand the effects of the point mutations on the structure of the IL-36Ra chimeras, we also solved the crystal structure of the double-swapped IL-36Ra that contains the two point mutations IL-36Ra(β4/5|β11/12)$^{R103A/M105A}$. These two mutations did not alter the local structure of the chimeric IL-36Ra when compared with the double-swapped IL-36Ra. Based on our complex model of IL-36R/IL-36Ra, these residues do not interact with IL-36R, but an electrostatic analysis revealed that the removal of Arg^{103} increases the negative charge in this region of IL-36Ra (Supplemental Fig. 2E, Supplemental Table I). However, because we can only measure binding to a preformed IL-36R/IL-1RAcP complex, we cannot distinguish whether these point mutations affect binding to IL-36R or IL-1RAcP or both.

IL-36 fusion chimeras

IL-1RI has two major sites for binding IL-1β and IL-1Ra. Site I is formed by the combined surface of D1 and D2, whereas site II is formed by D3. Whereas IL-1β binds to both sites I and II, IL-1Ra primarily engages site I. This lack of binding to site II enables a rotation of D3 away from the interface with IL-1RAcP, likely contributing to the antagonistic properties of IL-1Ra (21). Hou et al. (12) capitalized on the knowledge that IL-1Ra has a higher affinity for site I and IL-1β for site II to create IL-1β/IL-1Ra chimeras that combine both binding sites and function as either superior agonists or antagonists. To test whether IL-36γ and IL-36Ra behave similarly to the IL-1 cytokines, we generated chimeras of IL-36γ and IL-36Ra that corresponded to the most agonistic and antagonist chimeric version of IL-1β /IL-1Ra (Supplemental Fig. 1). Chimera 125:30 combines 125 residues from IL-36γ with 30 from IL-36Ra and corresponds to the superior agonist created by Hou et al. (12), whereas the superior antagonist chimera 96:63 combines 96 residues from IL-36γ and 63 from IL-36Ra. Surprisingly, both IL-36 chimeras had a much lower affinity than did either wild-type IL-36γ or IL-36Ra for the IL-36R/IL-1RAcP complex (Fig. 6C). This loss in affinity was also reflected in an almost complete loss in agonist potency and no measurable antagonist activity for both chimeras (Fig. 6A, 6B). Although IL-1β and IL-1Ra bind in an identical orientation to both IL-1RI and IL-1RII, the orientation of IL-33 bound to ST2 is slightly rotated (33), revealing that variability in the relative orientations of receptor, accessory protein, and IL to one another between IL-1 and IL-33 receptor systems exists. Our data suggest that 1) the orientation of IL-36 cytokines relative to the IL-36R differs from that of IL-1 cytokines to IL-1RI/II, and/or 2) IL-36γ and IL-36Ra do not bind identically to IL-36R (Fig. 7). Thus, although the molecular basis for signaling in the IL-1 and IL-36 receptor systems may be grossly similar, the fine specificities of agonist and antagonist cytokines are distinct (Fig. 8).

IL-36Ra mutations associated with generalized pustular psoriasis

After the initial reports of missense mutations in IL36RN (the gene coding for IL-36Ra) leading to generalized pustular psoriasis (17, 18), several other missense mutations have been identified (38–43). Altogether, 11 missense mutations of nine different residues have been reported to date (Table I). These residues can be subdivided into surface-exposed and buried residues. Mutations in the buried residues likely resulted in improper folding and reduced stability of IL-36Ra. All of the remaining, surface-exposed, residues are positioned at the putative interface with IL-36R and, thus, likely affect interactions between IL-36Ra and IL-36R. Two of the missense mutations (N47S and R48W) are located in the β4/5 loop, which we have shown is critical for the antagonistic activity of IL-36Ra.

Discussion

Through a combination of biophysical, functional, and structural analyses of the IL-36R–specific agonist IL-36γ, its antagonist IL-

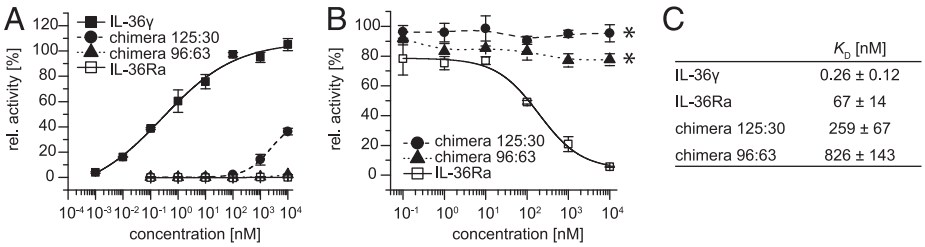

C

	K_D [nM]
IL-36γ	0.26 ± 0.12
IL-36Ra	67 ± 14
chimera 125:30	259 ± 67
chimera 96:63	826 ± 143

FIGURE 6. Construction of superior agonists and antagonists chimeras is not directly adoptable from the IL-1β/IL-1Ra system. We created chimeras of IL-36γ and IL-36Ra in analogy to the superior agonistic and antagonistic IL-1β/IL-1Ra chimeras described by Hou et al. (12). Chimera 125:30 corresponds to the superior agonist, chimera 96:63 to the superior antagonist. (**A**) Activation and (**B**) inhibition of IL-36R signaling was measured in the HEK293 T reporter cell system as outlined in Fig. 2. Data are the means of duplicates ± SD. One representative experiment of three replicates is shown. All data were fit to a four-parameter function, except those indicated with an asterisk. (**C**) Dissociation constants of chimeras and wild-type proteins as measure by SPR by binding to heterodimeric IL-36R/IL-1RAcP. Data are the means of at least four experiments ± SD (exact number of replicates is given in Supplemental Table II).

36Ra, and chimeras of the two, we have substantially defined the molecular mechanisms of agonism and antagonism in the IL-36 family. The IL-36 cytokines share the same coreceptor (IL-1RAcP) with the IL-1 cytokines and IL-33 and their respective primary receptors (7). Additionally, although the ILs and their receptors share the same fold, they have low sequence identity. In the two ternary structures of IL-1RAcP with IL-1RI/IL-1β and IL-1RII/IL-1β, the specific interactions of IL-1RAcP with IL-1β are identical, but only a subset of the interactions of IL-1RAcP with IL-1RI and IL-1RII is conserved (20, 21). Nevertheless, the overall architecture of these complexes is highly similar. Although the sequences of ST2 (IL-33R) and IL-36R also differ substantially from IL-1RI and IL-1RII, it is expected that the ternary complexes with IL-1RAcP exhibit the same architecture, as they use the same signaling cascade downstream of their intracellular Toll/IL-1 receptor domains (6). Because none of the ternary complexes involving IL-33 or any of the IL-36 cytokines has been resolved to date, the conservation of the ternary architecture of these complexes has only been assumed. In the present study, we have shown that agonism in the IL-36 subfamily follows grossly similar principles as in the IL-1 subfamily, but must employ distinct specific interactions for activation. Likewise, although the mode of action of antagonism in both IL-1 and IL-36 systems is similar, the precise molecular mechanisms by which antagonism is achieved differ markedly (Fig. 8).

First, we probed the general architecture of the ternary complex by introducing charge-switching point mutations at a position close to the C terminus of the ILs. In IL-1β, the aspartate at this position makes a hydrogen bond to IL-1RAcP Ser^{185} in both ternary complex crystal structures (20, 21), and switching this residue to lysine (the corresponding residue found in IL-1Ra) greatly reduced the potency of IL-1β (31). The reverse mutation in IL-1Ra renders the antagonist into a partial agonist (31). Although IL-36γ has an alanine at this position, IL-36α (aspartate) and IL-36β (asparagine) are both capable of forming a hydrogen bond. Introducing aspartate in IL-36γ increases the affinity to the IL-36R/IL-1RAcP receptor pair. Indeed, changing this residue to lysine greatly reduces the potency of IL-36γ, similar to what is observed for IL-1β (31), indicating that the general architecture of the ternary complex would allow the formation of the critical hydrogen bond between IL-1RAcP and IL-36. Additionally, based on the loop-swapping experiments, loop β11/12 seems to have the biggest contribution to the potential of IL-36γ, as the effects of swapping loops β4/5 on the agonist potency were less severe.

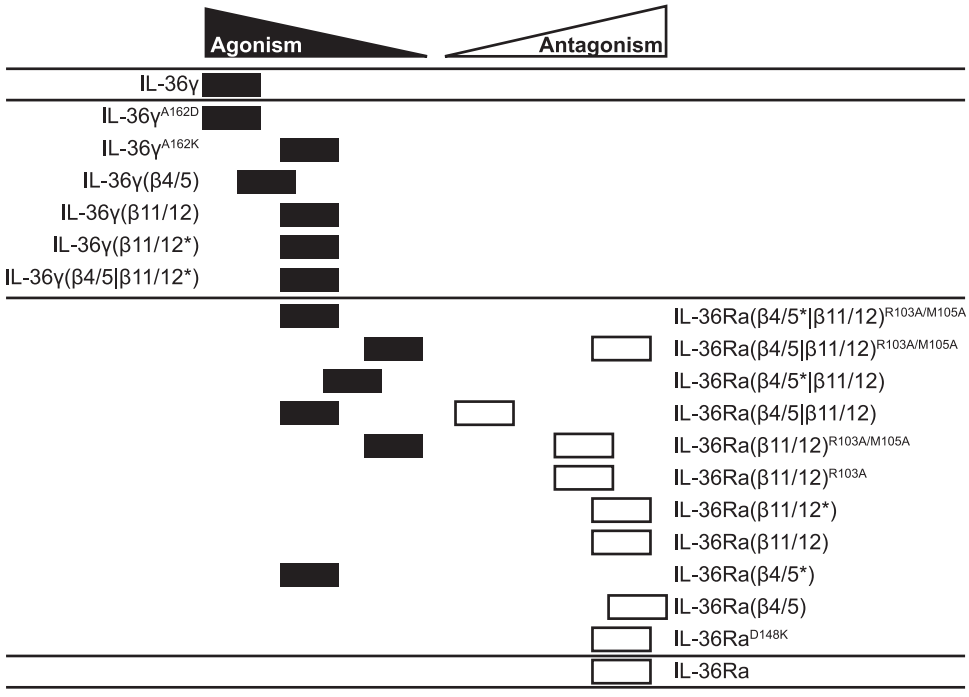

FIGURE 7. Summary of results from the IL-36 signal activation and inhibition assays. The ability of all analyzed variants of IL-36γ and IL-36Ra to activate or inhibit IL-36R–mediated signaling was related to their corresponding wild-type IL to enable comparison of all variants. Agonistic potential is symbolized as filled bars, whereas antagonistic potential is depicted as open bars. Relative agonist potency decreases from the left to the middle, whereas relative antagonistic potency decreases from the right to the middle.

Table I. Missense mutations associated with general pustular psoriasis

Mutation	Accessibility	Predicted Effect	References
L27P	Exposed	Interface with D1/D2 of IL-36R; reduced stability	(17, 38)
H32R	Exposed	Interface with D1/D2 of IL-36R; reduced binding	(41)
K35R	Exposed	Interface with D1/D2 of IL-36R; reduced binding	(39)
N47S	Buried	β4/5 loop, modulation of β4/5 and β7/8 loop conformation	(40)
R48W	Exposed	β4/5 loop/interface with D3 of IL-36R	(18, 38, 41)
P76L	Buried	Reduced stability/improper folding	(40, 41)
R102Q	Exposed	Interface with D3 of IL-36R, reduced binding	(40)
R102W	Exposed	Interface with D3 of IL-36R, reduced binding	(39)
S113L	Buried	Reduced stability/improper folding	(18, 38, 39, 41)
T123R	Buried	Reduced stability/improper folding	(43)
T123M	Buried	Reduced stability/improper folding	(42)

The basis for antagonism through IL-36Ra differs even more significantly from that of IL-1Ra. Most strikingly, the IL-36Ra β11/12 loop is much longer than those in IL-36α, IL-36β, and IL-36γ and likely acts to sterically hinder interaction with IL-1RAcP (Fig. 8). For the antagonistic properties of IL-1Ra the lysine directly C-terminal of the β11/12 loop is of utmost importance (31). IL-36Ra has an aspartate at this position, potentially enabling direct interaction with IL-1RAcP. However, this residue is likely shielded by the longer β11/12 loop. Although our binding assay does not enable us to discriminate between the individual contributions of IL-36R and IL-1RAcP to binding of IL-36γ and IL-36Ra, we observed a significant difference between the agonistic IL-36γ and the antagonistic IL-36Ra in their affinities for the IL-36R/IL-1RAcP heterodimer. Kinetically, these interactions exhibit similar association rates but differ greatly in their dissociation rates, resulting in a >250-fold relative change in affinity for the IL-36R/IL-1RAcP complex. The half-lives of the antagonistic complexes are therefore much shorter, which may be insufficient to bring the intracellular domains of IL-36R and IL-1RAcP long enough together to initiate signaling.

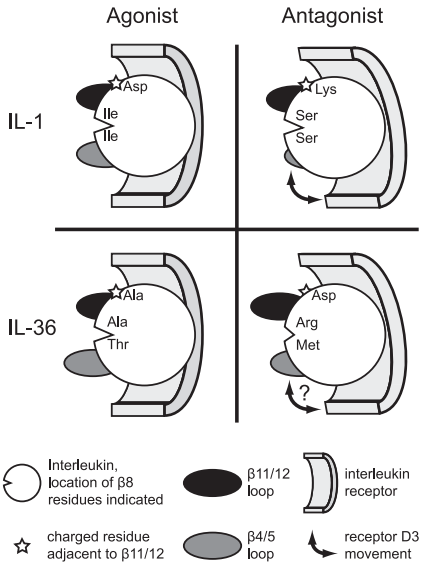

FIGURE 8. Agonism and antagonism of IL-1 and IL-36 signaling share common principles but differ in their details. Important difference between the agonist and antagonist for IL-1R are the length of the β4/5 loop and a residue adjacent to the β11/12 loop. In IL-1Ra, the shorter β4/5 loop causes a movement of the membrane-proximal D3 receptor domain away from the binding site of IL-1RAcP. The lysine residue adjacent to the β11/12 loop is not able to form an important hydrogen bond with IL-1RAcP that is mediated by aspartate at the same position in agonistic IL-1β. In the agonists for IL-36R this residue plays the same role. Although IL-36γ has an alanine at this position, changing this residue to the corresponding amino acids found in the IL-1 system had the same effect, indicating that the general architecture of the ternary complex of IL-R/IL/IL-1RAcP is maintained. In contrast, in IL-36Ra, this residue is aspartate as observed in the agonistic IL-1β. However, it is likely occluded from direct interaction with IL-1RAcP by the substantially longer β11/12 loop, which is likely also sterically hindering binding to IL-1RAcP. Loop β4/5 of the antagonist is shorter than the corresponding loops in the IL-36 agonists. This loop contributes significantly to the antagonistic properties of IL-36Ra, potentially by modulating movement of the IL-36R D3 domain. Additionally, the large side chains of Arg^{103} and Met^{105} on the β8 strand hinder the insertion of a helix of IL-1RAcP, which is critical for formation of a hydrogen bond adjacent to the β11/12 loop in the agonistic ILs.

Because the molecular details of the interactions of IL-36 cytokines with IL-36R and IL-1RAcP have not yet been described in atomic detail, it remains a challenge to rationally switch IL-36 agonists into complete antagonists and vice versa. Using the ternary IL-1β complex as a blueprint, simultaneous swapping of loops β4/5 and β11/12 in IL-36γ with those from IL-36Ra was not sufficient to remove all agonist potency (Fig. 7). This indicates that there are additional regions of IL-36γ that participate in binding to IL-1RAcP. Alternatively, simply swapping the extended β4/5 loop of IL-36γ into IL-36Ra was adequate to switch IL-36Ra from a complete antagonist into a partial agonist with no remaining antagonist activity. This chimera, however, had a comparatively low affinity and, therefore, had a much lower potency than did wild-type IL-36γ.

Our inability to create superior agonists and antagonists by creating chimeras of the putative binding sites for the D1/2 and D3 domains, in analogy to the strategy used for IL-1β and IL-1Ra (12), indicates that the IL-36 subfamily differs markedly from the IL-1 subfamily in the molecular mechanisms by which they activate and inhibit signaling. Through our mutational and loop-swapping experiments, we observed that the affinity of both the agonist IL-36γ (by mutation $Ala^{162}Asp$) and the IL-36Ra (by loop swap of β4/5 from IL-36γ) can be improved and, at least in the case of IL-36Ra, this also resulted in better antagonism. To rationally design superior agonists and antagonists for IL-36R, however, will require more insight into the precise molecular interactions of IL-36R binding to both its agonist and antagonist cytokines.

Acknowledgments

We thank Robert Beadenkopf, Beatriz Trastoy, Amanda Bowers, and Greg Snyder for help with cell culture, binding assay development, and crystallographic data collection. We thank beam line scientists at 23-ID-D and 23-ID-B, Advanced Photon Source, and at 11-1 and 12-2, Stanford Synchrotron Radiation Lightsource.

Disclosures

The authors have no financial conflicts of interest.

References

1. Lomedico, P. T., U. Gubler, C. P. Hellmann, M. Dukovich, J. G. Giri, Y. C. Pan, K. Collier, R. Semionow, A. O. Chua, and S. B. Mizel. 1984. Cloning and expression of murine interleukin-1 cDNA in *Escherichia coli*. *Nature* 312: 458–462.
2. Auron, P. E., A. C. Webb, L. J. Rosenwasser, S. F. Mucci, A. Rich, S. M. Wolff, and C. A. Dinarello. 1984. Nucleotide sequence of human monocyte interleukin 1 precursor cDNA. *Proc. Natl. Acad. Sci. USA* 81: 7907–7911.
3. Dinarello, C. A., A. Simon, and J. W. van der Meer. 2012. Treating inflammation by blocking interleukin-1 in a broad spectrum of diseases. *Nat. Rev. Drug Discov.* 11: 633–652.
4. Dinarello, C. A. 2009. Immunological and inflammatory functions of the interleukin-1 family. *Annu. Rev. Immunol.* 27: 519–550.
5. van de Veerdonk, F. L., A. K. Stoeckman, G. Wu, A. N. Boeckermann, T. Azam, M. G. Netea, L. A. Joosten, J. W. van der Meer, R. Hao, V. Kalabokis, and C. A. Dinarello. 2012. IL-38 binds to the IL-36 receptor and has biological effects on immune cells similar to IL-36 receptor antagonist. *Proc. Natl. Acad. Sci. USA* 109: 3001–3005.
6. O'Neill, L. A. 2008. The interleukin-1 receptor/Toll-like receptor superfamily: 10 years of progress. *Immunol. Rev.* 226: 10–18.
7. Sims, J. E., and D. E. Smith. 2010. The IL-1 family: regulators of immunity. *Nat. Rev. Immunol.* 10: 89–102.
8. Towne, J. E., B. R. Renshaw, J. Douangpanya, B. P. Lipsky, M. Shen, C. A. Gabel, and J. E. Sims. 2011. Interleukin-36 (IL-36) ligands require processing for full agonist (IL-36α, IL-36β, and IL-36γ) or antagonist (IL-36Ra) activity. *J. Biol. Chem.* 286: 42594–42602.
9. Vigne, S., G. Palmer, C. Lamacchia, P. Martin, D. Talabot-Ayer, E. Rodriguez, F. Ronchi, F. Sallusto, H. Dinh, J. E. Sims, and C. Gabay. 2011. IL-36R ligands are potent regulators of dendritic and T cells. *Blood* 118: 5813–5823.
10. Mutamba, S., A. Allison, Y. Mahida, P. Barrow, and N. Foster. 2012. Expression of IL-1Rrp2 by human myelomonocytic cells is unique to DCs and facilitates DC maturation by IL-1F8 and IL-1F9. *Eur. J. Immunol.* 42: 607–617.
11. Vigne, S., G. Palmer, P. Martin, C. Lamacchia, D. Strebel, E. Rodriguez, M. L. Olleros, D. Vesin, I. Garcia, F. Ronchi, et al. 2012. IL-36 signaling amplifies Th1 responses by enhancing proliferation and Th1 polarization of naive $CD4^+$ T cells. *Blood* 120: 3478–3487.
12. Hou, J., S. A. Townson, J. T. Kovalchin, A. Masci, O. Kiner, Y. Shu, B. M. King, E. Schirmer, K. Golden, C. Thomas, et al. 2013. Design of a superior cytokine antagonist for topical ophthalmic use. *Proc. Natl. Acad. Sci. USA* 110: 3913–3918.
13. Blumberg, H., H. Dinh, E. S. Trueblood, J. Pretorius, D. Kugler, N. Weng, S. T. Kanaly, J. E. Towne, C. R. Willis, M. K. Kuechle, et al. 2007. Opposing activities of two novel members of the IL-1 ligand family regulate skin inflammation. *J. Exp. Med.* 204: 2603–2614.
14. Tortola, L., E. Rosenwald, B. Abel, H. Blumberg, M. Schäfer, A. J. Coyle, J. C. Renauld, S. Werner, J. Kisielow, and M. Kopf. 2012. Psoriasiform dermatitis is driven by IL-36-mediated DC-keratinocyte crosstalk. *J. Clin. Invest.* 122: 3965–3976.
15. Debets, R., J. C. Timans, B. Homey, S. Zurawski, T. R. Sana, S. Lo, J. Wagner, G. Edwards, T. Clifford, S. Menon, et al. 2001. Two novel IL-1 family members, IL-1δ and IL-1ε, function as an antagonist and agonist of NF-κB activation through the orphan IL-1 receptor-related protein 2. *J. Immunol.* 167: 1440–1446.
16. Zhou, X., J. G. Krueger, M. C. Kao, E. Lee, F. Du, A. Menter, W. H. Wong, and A. M. Bowcock. 2003. Novel mechanisms of T-cell and dendritic cell activation revealed by profiling of psoriasis on the 63,100-element oligonucleotide array. *Physiol. Genomics* 13: 69–78.
17. Marrakchi, S., P. Guigue, B. R. Renshaw, A. Puel, X. Y. Pei, S. Fraitag, J. Zribi, E. Bal, C. Cluzeau, M. Chrabieh, et al. 2011. Interleukin-36-receptor antagonist deficiency and generalized pustular psoriasis. *N. Engl. J. Med.* 365: 620–628.
18. Onoufriadis, A., M. A. Simpson, A. E. Pink, P. Di Meglio, C. H. Smith, V. Pullabhatla, J. Knight, S. L. Spain, F. O. Nestle, A. D. Burden, et al. 2011. Mutations in *IL36RN/IL1F5* are associated with the severe episodic inflammatory skin disease known as generalized pustular psoriasis. *Am. J. Hum. Genet.* 89: 432–437.
19. Ramadas, R. A., S. L. Ewart, Y. Iwakura, B. D. Medoff, and A. M. LeVine. 2012. IL-36α exerts pro-inflammatory effects in the lungs of mice. *PLoS ONE* 7: e45784.
20. Thomas, C., J. F. Bazan, and K. C. Garcia. 2012. Structure of the activating IL-1 receptor signaling complex. *Nat. Struct. Mol. Biol.* 19: 455–457.
21. Wang, D., S. Zhang, L. Li, X. Liu, K. Mei, and X. Wang. 2010. Structural insights into the assembly and activation of IL-1β with its receptors. *Nat. Immunol.* 11: 905–911.
22. Towne, J. E., K. E. Garka, B. R. Renshaw, G. D. Virca, and J. E. Sims. 2004. Interleukin (IL)-1F6, IL-1F8, and IL-1F9 signal through IL-1Rrp2 and IL-1RAcP to activate the pathway leading to NF-κB and MAPKs. *J. Biol. Chem.* 279: 13677–13688.
23. Dunn, E. F., N. J. Gay, A. F. Bristow, D. P. Gearing, L. A. O'Neill, and X. Y. Pei. 2003. High-resolution structure of murine interleukin 1 homologue IL-1F5 reveals unique loop conformations for receptor binding specificity. *Biochemistry* 42: 10938–10944.
24. Li, C., A. Wen, B. Shen, J. Lu, Y. Huang, and Y. Chang. 2011. FastCloning: a highly simplified, purification-free, sequence- and ligation-independent PCR cloning method. *BMC Biotechnol.* 11: 92.
25. Huang, J., X. Gao, S. Li, and Z. Cao. 1997. Recruitment of IRAK to the interleukin 1 receptor complex requires interleukin 1 receptor accessory protein. *Proc. Natl. Acad. Sci. USA* 94: 12829–12832.
26. Kabsch, W. 2010. XDS. *Acta Crystallogr. D Biol. Crystallogr.* 66: 125–132.
27. Evans, P. R., and G. N. Murshudov. 2013. How good are my data and what is the resolution? *Acta Crystallogr. D Biol. Crystallogr.* 69: 1204–1214.
28. McCoy, A. J., R. W. Grosse-Kunstleve, P. D. Adams, M. D. Winn, L. C. Storoni, and R. J. Read. 2007. Phaser crystallographic software. *J. Appl. Cryst.* 40: 658–674.
29. Adams, P. D., P. V. Afonine, G. Bunkóczi, V. B. Chen, I. W. Davis, N. Echols, J. J. Headd, L. W. Hung, G. J. Kapral, R. W. Grosse-Kunstleve, et al. 2010. PHENIX: a comprehensive Python-based system for macromolecular structure solution. *Acta Crystallogr. D Biol. Crystallogr.* 66: 213–221.
30. Emsley, P., B. Lohkamp, W. G. Scott, and K. Cowtan. 2010. Features and development of *Coot*. *Acta Crystallogr. D Biol. Crystallogr.* 66: 486–501.
31. Ju, G., E. Labriola-Tompkins, C. A. Campen, W. R. Benjamin, J. Karas, J. Plocinski, D. Biondi, K. L. Kaffka, P. L. Kilian, S. P. Eisenberg, et al. 1991. Conversion of the interleukin 1 receptor antagonist into an agonist by site-specific mutagenesis. *Proc. Natl. Acad. Sci. USA* 88: 2658–2662.
32. Greenfeder, S. A., T. Varnell, G. Powers, K. Lombard-Gillooly, D. Shuster, K. W. McIntyre, D. E. Ryan, W. Levin, V. Madison, and G. Ju. 1995. Insertion of a structural domain of interleukin (IL)-1β confers agonist activity to the IL-1 receptor antagonist. Implications for IL-1 bioactivity. *J. Biol. Chem.* 270: 22460–22466.
33. Liu, X., M. Hammel, Y. He, J. A. Tainer, U. S. Jeng, L. Zhang, S. Wang, and X. Wang. 2013. Structural insights into the interaction of IL-33 with its receptors. *Proc. Natl. Acad. Sci. USA* 110: 14918–14923.
34. Vigers, G. P., D. J. Dripps, C. K. Edwards, III, and B. J. Brandhuber. 2000. X-ray crystal structure of a small antagonist peptide bound to interleukin-1 receptor type 1. *J. Biol. Chem.* 275: 36927–36933.
35. Eswar, N., B. John, N. Mirkovic, A. Fiser, V. A. Ilyin, U. Pieper, A. C. Stuart, M. A. Marti-Renom, M. S. Madhusudhan, B. Yerkovich, and A. Sali. 2003. Tools for comparative protein structure modeling and analysis. *Nucleic Acids Res.* 31: 3375–3380.
36. Schreuder, H., C. Tardif, S. Trump-Kallmeyer, A. Soffientini, E. Sarubbi, A. Akeson, T. Bowlin, S. Yanofsky, and R. W. Barrett. 1997. A new cytokine-receptor binding mode revealed by the crystal structure of the IL-1 receptor with an antagonist. *Nature* 386: 194–200.
37. Vigers, G. P., L. J. Anderson, P. Caffes, and B. J. Brandhuber. 1997. Crystal structure of the type-I interleukin-1 receptor complexed with interleukin-1β. *Nature* 386: 190–194.
38. Navarini, A. A., L. Valeyrie-Allanore, N. Setta-Kaffetzi, J. N. Barker, F. Capon, D. Creamer, J. C. Roujeau, P. Sekula, M. A. Simpson, R. C. Trembath, et al. 2013. Rare variations in IL36RN in severe adverse drug reactions manifesting as acute generalized exanthematous pustulosis. *J. Invest. Dermatol.* 133: 1904–1907.
39. Setta-Kaffetzi, N., A. A. Navarini, V. M. Patel, V. Pullabhatla, A. E. Pink, S. E. Choon, M. A. Allen, A. D. Burden, C. E. Griffiths, M. M. Seyger, et al. 2013. Rare pathogenic variants in *IL36RN* underlie a spectrum of psoriasis-associated pustular phenotypes. *J. Invest. Dermatol.* 133: 1366–1369.
40. Li, M., J. Han, Z. Lu, H. Li, K. Zhu, R. Cheng, Q. Jiao, C. Zhang, C. Zhu, Y. Zhuang, et al. 2013. Prevalent and rare mutations in IL-36RN gene in Chinese patients with generalized pustular psoriasis and psoriasis vulgaris. *J. Invest. Dermatol.* 133: 2637–2639.
41. Körber, A., R. Mössner, R. Renner, H. Sticht, D. Wilsmann-Theis, P. Schulz, M. Sticherling, H. Traupe, and U. Hüffmeier. 2013. Mutations in IL36RN in patients with generalized pustular psoriasis. *J. Invest. Dermatol.* 133: 2634–2637.
42. Kanazawa, N., T. Nakamura, N. Mikita, and F. Furukawa. 2013. Novel *IL36RN* mutation in a Japanese case of early onset generalized pustular psoriasis. *J. Dermatol.* 40: 749–751.
43. Farooq, M., H. Nakai, A. Fujimoto, H. Fujikawa, A. Matsuyama, N. Kariya, A. Aizawa, H. Fujiwara, M. Ito, and Y. Shimomura. 2013. Mutation analysis of the *IL36RN* gene in 14 Japanese patients with generalized pustular psoriasis. *Hum. Mutat.* 34: 176–183.

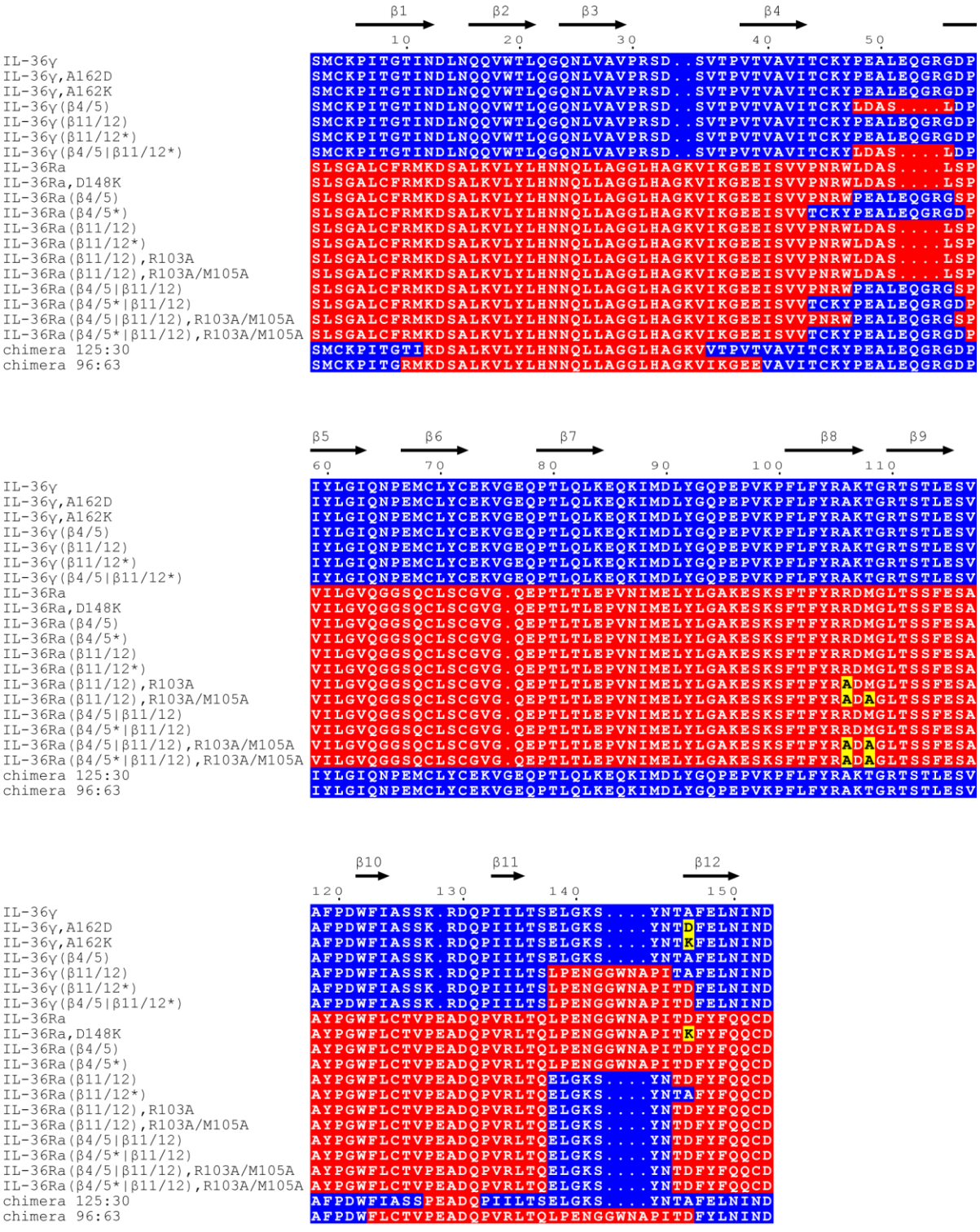

Supplementary Figure 1: Sequence alignments of proteins used in the present study. Parts derived from IL-36γ are blue, parts derived from IL-36Ra are red. Point mutations are highlighted in yellow. Position of the twelve β strands of the β trefoil fold are indicated as observed in the structure of IL-36γ.

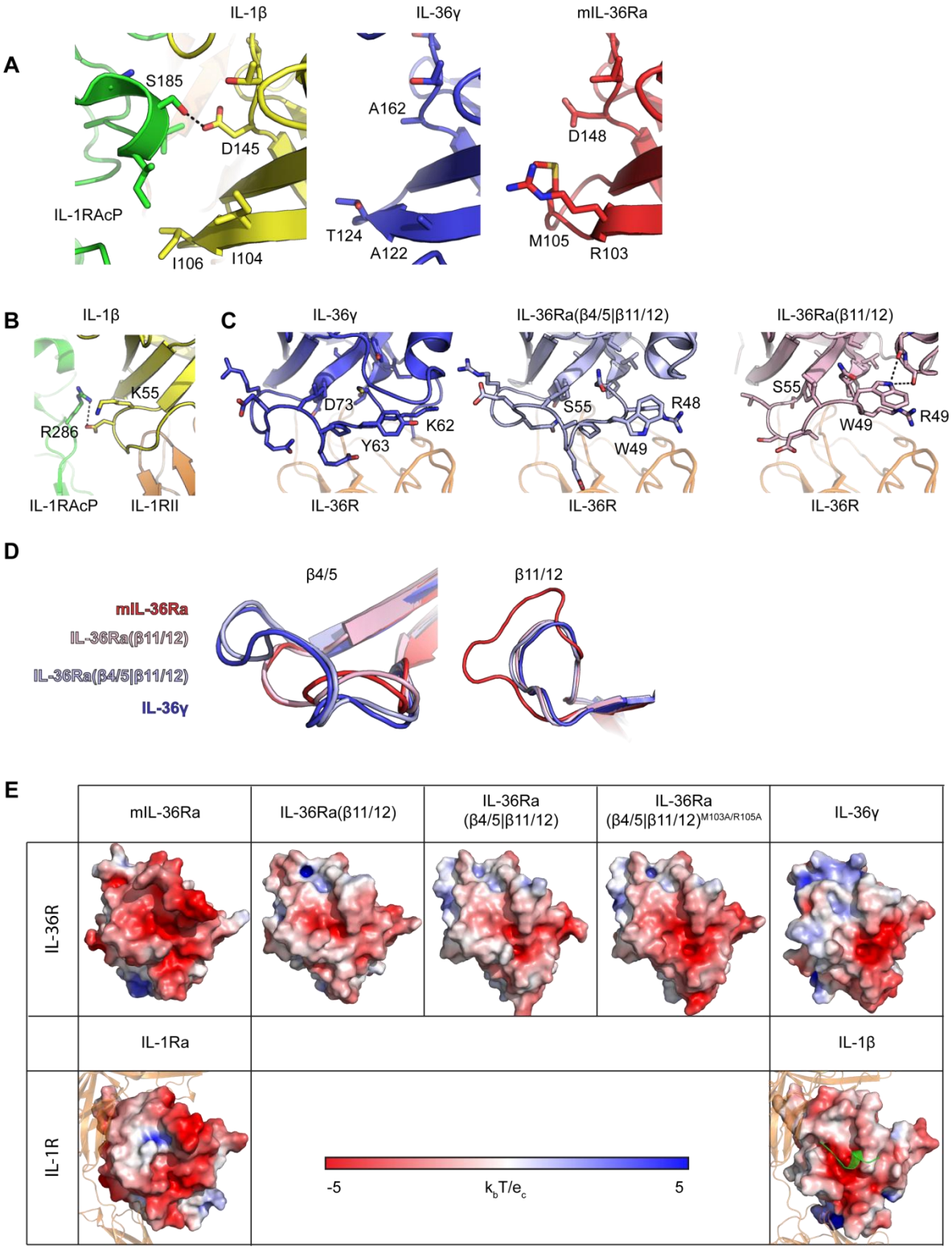

Supplementary Figure 2: Crystal structures of IL-36γ and loop swapped IL-36Ra. **(A)** Left, hydrogen bond between IL-1RAcP/S185 and IL-1β/D145 as observed in PDB 3O4O and same region in structures of IL-36γ (middle) and murine IL-36Ra (right, PDB 1MD6). **(B)** Interaction of loops β4/5 of IL-1β with IL-1RAcP (PDB 3O4O). **(C)** Interface of IL-36γ, IL-36Ra(β11/12) and IL-36Ra(β4/5| β11/12) with a homology model of the domain D3 of IL-36R. Residues within the loop are depicted as sticks. **(D)** Conformation of loops swapped from IL-36γ into IL-36Ra as observed in the crystal structures of murine IL-36Ra, IL-36γ, single loops swapped IL-36Ra(β11/12) and IL-36Ra(β4/5|β11/12). **(E)** Electrostatic potential of agonistic and antagonistic IL-36s. Wild type and chimeric IL-36Ra and IL-36γ are shown as surface models with their electrostatic potential calculated with APBS onto their surface. Orientation is the same as for IL-Ra (PDB 1IRA) and IL-1β (PDB 3O4O), basically showing the side of the interleukin that face IL-1RAcP. Position of IL-1RI and helix of IL-1RAcP that interacts with IL-1β are shown as cartoons in the lower row. Red corresponds to a surface potential of -5 kT/e and blue of +5 kT/e, respectively. Surface potentials were calculated using the program APBS [Baker, NA, Sept D, Joseph S, McCammon JA (2001) Electrostatics of nanosystems: Application to microtubules and the ribosome. Proc Natl Acad Sci USA 98:10037–10041].

	IL-36γ	IL-36Ra (β11/12)	IL-36Ra (β4/5|β11/12)	IL-36Ra (β4/5|β11/12)$^{R103A/M105A}$
Data collection				
Resolution range (Å)	34.9-2.0 (2.11-2.0)*	29.2-2.3 (2.37-2.3)	37.3-1.7 (1.73-1.7)	37-1.55 (1.58-1.55)
Space group	P 43 21 2	P 1	P 31 2 1	P 31 2 1
Unit cell				
a, b, c (Å)	89.3 89.3 37.9	41.4 41.5 50.8	43.1 43.1 119.1	42.8 42.8 119.8
α, β, γ (°)	90 90 90	97.9 102.3 118.5	90 90 120	90 90 120
Total reflections	132409 (17029)	22761 (1492)	117020 (5540)	183258 (8548)
Unique reflections	10707 (1492)	11902 (852)	14865 (782)	19268 (913)
Multiplicity	12.4 (11.4)	1.9 (1.8)	7.9 (7.1)	9.5 (9.4)
Completeness (%)	99.1 (97.2)	95.0 (70.0)	99.9 (99.1)	99.9 (98.8)
Mean I/sigma(I)	25.0 (6.2)	3.9 (0.9)	14.8 (2.2)	20.5 (2.8)
Wilson B-factor	21.72	38.46	18.49	17.12
R_{merge} (%)	9.8 (58.5)	8.3 (58.4)	9.1 (83.7)	6.5 (73.5)
R_{meas} (%)	10.2 (61.3)	11.7 (82.6)	9.8 (90.3)	6.5 (77.7)
CC1/2	0.999 (0.919)	0.988 (0.59)	0.999 (0.737)	1 (0.86)
Data refinement				
R_{work}/R_{free} (%)	17.8/22.5	21/23.9	19.5/23.3	18.1/21.5
Number of non-hydrogen atoms	1291	2318	1247	1298
macromolecules	1181	2266	1124	1159
water	110	52	123	139
protein residues	152	294	144	143
RMS(bonds)	0.007	0.003	0.007	0.013
RMS(angles)	1.18	0.87	1.08	1.44
Ramachandran favored (%)	97	96	96	97
Ramachandran outliers (%)	0.67	0	0	0
Average B-factor	19.40	45.30	25.90	23.50
macromolecules	18.90	45.40	25.30	22.70
solvent	24.40	39.60	30.80	30.40

*Statistics for the highest-resolution shell are shown in parentheses.

Supplementary Table I: X-ray data collection and refinement

				normalized to wt			
	k_a [1/Ms]	k_d [1/s]	K_D [nM]	$k_{a,mut}/k_{a,wt}$	$k_{d,mut}/k_{d,wt}$	$K_{D,mut}/K_{D,wt}$	n
IL-36γ	$1.6 \pm 0.3 \times 10^5$	$3.8 \pm 1.5 \times 10^{-5}$	0.26 ± 0.12	1	1	1	12
IL-36γ^{A162D}	$4.1 \pm 0.6 \times 10^5$	$3.2 \pm 1 \times 10^{-5}$	0.08 ± 0.04	2.6	0.8	0.3	6
IL-36γ^{A162K}	$6 \pm 3 \times 10^5$	$1.5 \pm 0.6 \times 10^{-2}$	26.8 ± 5.8	3.9	394	103	5
IL-36γ(β4/5)	$1.8 \pm 0.2 \times 10^5$	$6.7 \pm 1.4 \times 10^{-5}$	0.38 ± 0.09	1.1	1.7	1.4	6
IL-36γ(β11/12)	$1.2 \pm 0.1 \times 10^5$	$4.3 \pm 0.2 \times 10^{-4}$	3.5 ± 0.4	0.8	11.2	13.6	4
IL-36γ(β11/12*)	$2.2 \pm 0.2 \times 10^5$	$1.1 \pm 0.1 \times 10^{-3}$	5.1 ± 0.6	1.4	28.8	19.5	4
IL-36γ(β4/5|β11/12*)	n.d.	n.d.	9045 ± 1834	n.d.	n.d.	34817	3
IL-36Ra	$5.1 \pm 1.3 \times 10^5$	$3.5 \pm 1.6 \times 10^{-2}$	67 ± 14	1	1	1	10
IL-36Ra^{D148K}	$5.9 \pm 2.8 \times 10^5$	$3.7 \pm 1.5 \times 10^{-2}$	65 ± 7	1.2	1.1	1	5
IL-36Ra(β4/5)	$2.9 \pm 0.3 \times 10^5$	$1.1 \pm 0.1 \times 10^{-2}$	36 ± 3	0.6	0.3	0.5	6
IL-36Ra(β4/5*)	n.d.	n.d.	4937 ± 877	n.d.	n.d.	74	2
IL-36Ra(β11/12)	$5 \pm 0.2 \times 10^5$	$6.1 \pm 2.6 \times 10^{-2}$	121 ± 45	1	1.8	1.8	3
IL-36Ra(β11/12*)	$5.3 \pm 0.4 \times 10^5$	$5.5 \pm 2.3 \times 10^{-2}$	103 ± 37	1	1.6	1.5	3
IL-36Ra(β11/12)^{R103A}	$4.8 \pm 0.5 \times 10^5$	$7.1 \pm 1.1 \times 10^{-2}$	146 ± 9	0.9	2	2.2	4
IL-36Ra(β11/12)$^{R103A/M105A}$	$7.2 \pm 2.1 \times 10^5$	$4 \pm 0.8 \times 10^{-2}$	59 ± 22	1.4	1.1	0.9	4
IL-36Ra(β4/5|β11/12)	$4.2 \pm 1.1 \times 10^5$	$2.9 \pm 0.6 \times 10^{-2}$	71 ± 5	0.8	0.8	1.1	5
IL-36Ra(β4/5*|β11/12)	n.d.	n.d.	16728 ± 2379	n.d.	n.d.	251	5
IL-36Ra(β4/5|β11/12)$^{R103A/M105A}$	$5.8 \pm 1.5 \times 10^5$	$1.8 \pm 0.3 \times 10^{-2}$	32 ± 4	1.1	0.5	0.5	5
IL-36Ra(β4/5*|β11/12)$^{R103A/M105A}$	n.d.	n.d.	2885 ± 713	n.d.	n.d.	43	5
chimera 125:30	n.d.	n.d.	259 ± 67				4
chimera 96:63	n.d.	n.d.	826 ± 143				4

n.d.) not determined, only equilibrium binding measured for this chimera

Supplementary Table II: Surface plasmon resonance data for binding of wt and chimeric interleukins to the heterodimer of IL-36R/IL-1RAcP